Spatial landslide susceptibility mapping using integrating an adaptive neuro-fuzzy inference system (ANFIS) with two multi-criteria decision-making approaches

Sina Paryani
Islamic Azad University Science and Research Branch
Aminreza Neshat (neshat.aminreza@srbiau.ac.ir)
Islamic Azad University Science and Research Branch https://orcid.org/0000-0001-9557-3570
Biswajeet Pradhan
Islamic Azad University Science and Research Branch

Research Article

Keywords: landslide susceptibility, machine learning, GIS, ANFIS, SWARA, BWM

Posted Date: March 10th, 2021

DOI: https://doi.org/10.21203/rs.3.rs-299575/v1

Version of Record: A version of this preprint was published at Theoretical and Applied Climatology on August 16th, 2021. See the published version at https://doi.org/10.1007/s00704-021-03695-w.

Spatial landslide susceptibility mapping using integrating an adaptive neuro-fuzzy inference system (ANFIS) with two multi-criteria decision-making approaches

Sina Paryani[a], Aminreza Neshat[a*], Biswajeet Pradhan[b,c]

[a] Department of GIS/RS, Faculty of Natural Resources and Environment, Science and Research Branch, Islamic Azad University, Tehran, Iran

[b] Centre for Advanced Modelling and Geospatial Information Systems (CAMGIS), Faculty of Engineering and IT, University of Technology Sydney, New South Wales, Australia

[c] Department of Energy and Mineral Resources Engineering, Choongmu-gwan, Sejong University, 209, Neungdong-roGwangin-gu, Seoul 05006, Korea

Correspondence:
Assistant Prof. Dr. Aminreza Neshat
Phone: +982122112144
Cell phone: +989121946646, +17783166646
Fax: +982122111603
Department of GIS/RS, Faculty of Natural Resources and Environment, Science and Research Branch, Islamic Azad University, Tehran, Iran
Email: neshat.aminreza@gmail.com, neshat.aminreza@srbiau.ac.ir
ORCID: https://orcid.org/0000-0001-9557-3570

Spatial landslide susceptibility mapping using integrating an adaptive neuro-fuzzy inference system (ANFIS) with two multi-criteria decision-making approaches

Abstract

Landslide is a type of slope processes causing a plethora of economic damage and loss of lives worldwide every year. This study aimed to analyze spatial landslide susceptibility mapping in the Khalkhal-Tarom Basin by integrating an adaptive neuro-fuzzy inference system (ANFIS) with two multi-criteria decision-making approaches, i.e. the stepwise weight assessment ratio analysis (SWARA) and the new best-worst method (BWM) techniques. For this purpose, the first step was to prepare a landslide inventory map, which were then divided randomly by the ratio of 30/70 for model training and validation. Thirteen conditioning factors were used as slope angle, slope aspect, altitude, topographic wetness index (TWI), plan curvature, profile curvature, distance to roads, distance to streams, distance to faults, lithology, land use, rainfall and normalized difference vegetation index (NDVI). After the database was created, the BWM and the SWARA methods were utilized to determine the relationships between the sub-criteria and landslides. Finally, landslide susceptibility maps were generated by implementing ANFIS-SWARA and ANFIS-BWM hybrid models, and the ROC curve was employed to appraise the predictive accuracy of each model. The results showed that the areas under curves (AUC) for the ANFIS-SWARA and ANFIS-BWM models were 73.6% and 75% respectively, and that the novel BWM yielded more realistic relationships between effective factors and the landslides. As a result, it was more efficient in training the ANFIS. Evidently, the generated landslide susceptibility maps (LSMs) can be very efficient in managing land use and preventing the damage caused by the landslide phenomenon.

Keywords: landslide susceptibility; machine learning; GIS; ANFIS; SWARA; BWM

Introduction

Causing great losses of lives and properties, landslides are dangerous processes that occur repeatedly in mountainous and hilly areas worldwide, (Juliev et al. 2019; Gutiérrez et al. 2015). This mass movement occurs whenever the loading of an earth material exceeds its shear strength (Lin et al. 2017). Although this geological phenomenon is often triggered by earthquakes and heavy rainfalls, the expansion of anthropogenic activities in susceptible areas has always played an important factor in its occurrence (Baena et al. 2019) Despite the

increased human knowledge regarding landslide occurrence and factors controlling this phenomenon, it is believed that the damage caused by landslides will increase due to deforestation, climate change and urban development (Pham and Prakash 2018). Therefore, it is essential to acquire accurate and realistic information about the spatial distribution and degrees of susceptibility for landslide-prone regions (Colkesen et al. 2016). To achieve this goal and to mitigate the destructive impacts of this phenomenon, landslide susceptibility maps can serve as an appropriate tool for increasing awareness and predicting future hazards (Feizizadeh et al. 2017). Based on previous landslides and identical physical features in similar areas, a landslide susceptibility map provides important signs regarding the locations where future landslides are likely to occur (Pradhan et al. 2017).

The Alborz Mountain has always been subject to the natural disasters such as landslide due to its being on the seismic belt of the Himalayas (Farrokhnia et al. 2011). In a study of identifying high-risk regions of the world with respect to landslide hazard, Nadim et al. (2006) reported that the Alborz and Zagros Mountains of Iran were among the areas with moderate to high landslide risks. In addition, according to the National Committee on Natural Disaster Reduction of the Iranian Ministry of Interior, the annual damage caused by landslides in Iran amounts to about 500 billion Rials (Arab Amiri et al. 2019). Consequently, if the loss of human life is taken into account, it is evident that zoning of the study area is necessary.

In the recent years, researchers have used different methods and their combinations to zone the areas susceptible to landslide in different areas worldwide that can generally classify into two quantitative and qualitative groups. The qualitative approaches, also known as knowledge-driven approaches, are the techniques of assigning weights to and rank criteria and sub-criteria based on experts' knowledge and experience and also on mathematical relations defined for each method. Some of these methods, which have been used in various studies and have yielded acceptable results, include the AHP (Zhang et al. 2016; Pourghasemi and Rossi 2017; Yan et al. 2019; Du et al. 2019) and hybrid methods such as MCDA and MCE (Kavzoglu et al. 2014; Erener et al. 2016; Kumar et al. 2017) and the WLC (Kouli et al. 2014; Ahmed 2015). The second group, also known as data-driven approaches, consists of the techniques which are not influenced by experts' opinions in the computational process. Instead, the relationship between the landslides and the effective parameters is determined by using probabilistic equations. These methods, which have been used repeatedly in various studies on landslides, include bivariate and multivariate probability models such as frequency ratio (FR) (Hong et al. 2017; Sharma and Mahajan 2018; Berhane et al., 2020), weight of evidence (WoE) (Kayastha et al. 2013; Ding et al. 2017; Cui et al. 2017) and logistic regression (LR) (Wang et al. 2015; Oh et

al. 2018; Pham et al. 2019) as well as soft computing methods such as artificial neural network (ANN) (Polykretis et al. 2014; Bui et al. 2016; Pham et al. 2017; Zhu et al. 2018; Moayedi et al. 2018), fuzzy logic (Pradhan et al. 2011; Ramesh and Anbazhagan 2015; Turan et al. 2020), adaptive neuro-fuzzy inference system (ANFIS) (Aghdam et al. 2017; Polykretis et al. 2019; Paryani et al. 2020), random forest (RF) (Kim et al. 2018) and support vector machine (SVM) (Pradhan 2013; Oh et al. 2018). According to the literature review, it is clear that although these models have effective performance in computational process, hybrid methods performs a strong structure to achieve more accurate results. Youssef et al. (2015) combined logistic regression and frequency ratio methods to landslide susceptibility mapping in Saudi Arabia. They concluded that ensemble of FR-LR model combining models has better results than using them alone. In another study, Aghdam et al. (2017) combined FR and WoE statistical methods with ANFIS algorithms to produce landslide susceptibility map of the Zagros Mountains in Iran. Their results indicated that FR-ANFIS and WoE-ANFIS have better performance compared with FR and WoE. It seems that using new methods is necessary to achieve more accurate results. Therefore, achieving optimal results relies on (a) the quality of the input data, (b) the structure of the model, used (Adineh et al. 2018).

In comparison with other studies, the research innovation of this study was to train the ANFIS method through the new multi-criteria decision-making method BWM (ANFIS-BWM) as a new hybrid model and compare it with the hybrid ANFIS-SWARA model. In other words, the weights obtained from BWM and SWARA methods were used as ANFIS input data. Landslide susceptibility maps were then generated for both models, and their performance accuracy was estimated by using the ROC curves. Finally, the results were compared to determine which of the two BWM and SWARA approaches were able to train the ANFIS network better and generate more realistic maps.

Study Region

With an area of 8604 km^2, the Khalkhal-Tarom Basin is located on the southern slopes of the Alborz mountain range along from 47^0 42′ 44″ to 49^0 10′ 34″ and 36^0 37′ 22″ to 37^0 56′ 35″ (Fig. 1). Approximately 92% (7967 km^2) of the Basin consists of highlands and the remainder of plains. The highest and lowest elevations are 3314 m and 288 m, respectively. The data from the climatological stations of Iran Meteorological Organization and Ministry of Energy were utilized to estimate temperature and precipitation. The average annual temperature in the region is about 10.5° C; while, the coldest month is February, and the warmest is August. In addition, the average annual rainfall is about 375 mm. The difference in precipitation levels in the

highlands on the two sides of the main river (the Ghezel Ozan River) results from the differences in the prevailing climatic conditions in the areas adjacent to the study area. Although the study area has diverse lithology, pyroclastic rocks of Karaj Formation cover most of its surface area. Regarding land use, range lands are the largest land cover class; however, agricultural lands and orchards cover nearly 16% of the land area in the basin and exhibit an increasing trend given the population increase. Given the existence of economic infrastructures and the growing residential areas in future, zoning of landslide-prone regions seems to be vitally important.

Database Development and Data Preparation

It is necessary to create database in any study of geographical information system. The landslide zoning is no exception, and database creation including inventory map and conditioning factors is considered as the first and the most important step in this process. The landslide inventory map shows the locations and spatial distribution of landslides that happened in the past. Since it is crucial to pinpoint the locations of the past and present landslides in order to predict future high-risk areas, preparation of a landslide inventory map is a requisite to any study on landslides (Regmi et al. 2013). Information on the locations of past landslides and their spatial distributions was obtained from the Forest, Rangeland and Watershed Organization of Iran (Fig. 1). According to Figure 1, the inventory map was employed to randomly select 172 (or 70%) of the 242 landslides that have occurred in the region for training the data and the 30% for model validation.

Various factors including geology, hydrology, geomorphology, climate and topography affect slope instability. Determination of these factors is among the basic, and initial steps in landslide zoning. In this study, thirteen conditioning factors including slope angle, slope aspect, altitude, topographic wetness index (TWI), plan curvature, profile curvature, distance to roads, distance to streams, distance to faults, lithology, land use, rainfall, normalized difference vegetation index (NDVI) were selected based on the characteristics of the study area, experts opinion and previous studies for the spatial modeling of the landslides (Table 1). According to Table 1, these thirteen factors were determined by using the information obtained from the related organizations and the reference data. Following that, ArcGIS was employed to generate and digitalize the maps (30-×30-m pixels). Raster data models of the layers were then prepared by using the selected methods.

In order to prepare the different information layers, the digital elevation model (DEM) was prepared first using ASTER satellite images. DEM is one of the most important databases in

any landslide study because preparation of some important thematic maps depends on it. The slope angle, slope aspect, altitude, TWI and plan and profile curvature layers were extracted from the DEM (Fig. 2 a-f). The other considered factors (distance to roads, distance to streams, distance to faults, lithology, land use, rainfall and the Normalized Difference Vegetation Index were then determined, respectively (Fig. 2 g-m). In addition, the conditioning factors were categorized based on experts' opinions, previous studies and study area characteristics.

The slope degree is always considered as an essential factor in analyzing the areas susceptible to landslide (Umar et al. 2014), because it is the major cause of mass movements. Exposure to sunlight, dry winds, and increased relative humidity due to rainfall are all factors associated with slope aspect that trigger landslides (Kavzoglu et al. 2013). Therefore, slope aspect has always been consideration by researchers. This factor is divided into 9 classes. Altitude is not directly involved in the occurrence of landslides; however, other factors related to it such as tectonic activity, weathering and climate change influence the entire process (Rozos et al. 2008). The topographic wetness index is a useful tool for estimating moisture conditions at basin scale (Grabs et al. 2009). This factor was used due to the varying humidity conditions in the study area. The values obtained from the slope curvature show the morphology of the different elevation points (Erener et al. 2010). In this paper, both the profile curvature curve and the plan curvature were taken into account. The former indicates the velocity and process of sediment transport and the second the divergence and convergence of the flow passing through the surface (Dehnavi et al. 2015). Road construction, especially when engineering principles are ignored, reduces slope stability and consequently triggers landslides (Moosavi and Niazi 2015). Therefore, the distance from the road has always attracted the interest of researchers (Xiao et al. 2019; Bui et al. 2012). Streams decrease shear strength by eroding the materials from the toe of the slope. Consequently, the factor of distance from the stream is very important in relation to slope stability (Achour et al. 2017). Faults, especially in seismic zones, play a significant role in triggering mass movements. They either act directly as a triggering factor for landslides or indirectly by causing fractures in slope layers that lead to the penetration of water into joints and fissures, thereby reducing the shear strength of materials constituting the slope that results in the occurrence of landslides. lithology as a geological factor has always been important role in predicting landslide occurrence probability because different lithologic units with varying degrees of permeability influence slope stability (Chalkias et al. 2014). Due to their impacts on slope instability, different types of land use have always attracted many researchers in their research on landslides (Conforti et al. 2013; Dou et al. 2014). The precipitation factor was used in this research because the amount of precipitation varies with

changes in elevation and precipitation directly and indirectly influences landslide occurrence. The NDVI index was calculated to analyze the effect of vegetation on slope instability:

$$NDVI = \frac{NIR-R}{NIR+R} \quad (1)$$

The NDVI benefits from the ratio of near-infrared (NIR) reflection to red (R) reflection to estimate vegetation density (Hall et al. 1995).

Methodology

Step-wise weight assessment ratio analysis (SWARA) model

This is a multi-criteria decision-making method with an ultimate objective like that of other similar approaches: assigning weights to criteria and sub-criteria. Since its introduction by Keršulien *et al.* in 2011, researchers have used it to analyze various areas (Mardani et al. 2015). An advantage of this method is its flexibility that allows experts to prioritize the criteria based on the existing conditions. The main feature of this approach is its capability in estimating experts' opinions in relation to the relative importance of the criteria in order to determine their weights (Keršulien et al. 2011). This procedure consists of the following steps:

1. Selecting the required criteria and ranking them according to their degrees of importance (the most important criteria take the highest position of ranking and the least important ones the lowest).
2. Calculating the coefficient K_j, which is a function of the relative importance of each criterion.
3. Determining the initial weight of each criterion.
4. Calculating the final normalized weight.

The final weight for each criterion is calculated through the following equations (Keršulien et al. 2011):

$$S_j = \frac{\sum_i^n A_i}{n} \quad (2)$$

In this equation, j and n represent the criterion number and the number of experts, respectively. The value of A_i also indicates the suggested rating of each criterion.

$$K_j = S_j + 1 \quad (3)$$

$$Q_j = \frac{X_j - 1}{K_j} \quad (4)$$

Here, K_j and Q_i are functions of the relative importance and initial weight of each criterion, respectively.

$$W_j = \frac{Q_j}{\sum_{j=1}^{m} Q_j} \quad (5)$$

In this formula, j represents the criterion number, and m shows the number of criteria when W_j indicates the final weight.

The final weight (W_j) obtained for each sub-criteria in this study indicates the relationship between landslides and conditioning factors. The larger/smaller the final weight of a sub-criterion is, the higher/lower its importance in landslide occurrence will be.

Best-worst multi-criteria decision making (BWM) model

The best-worst method (BWM) is one of the newest and most efficient multi-criteria decision-making approaches introduced in 2015 by Rezaei to calculate the final weights of criteria and sub-criteria in decision-making problems. As in other MCDM methods such as AHP, pair-wise comparisons are used in BWM. However, the differences in the final weight calculation in this method have made the final result much more realistic and consistent than methods such as AHP. The advantages of BWM over AHP are that fewer pair-wise comparisons are used, the numbers used for pair-wise comparisons are integers ranging between 1 and 9, and there is no need for fractional numbers. It is also possible to integrate the BWM with other MCDM methods (Ahmad et al. 2017). The various steps in this method and its algorithms for problem solving are as follows (Rezaei 2015):

1. Specifying the decision-making criteria for evaluation. The set of criteria is defined as $\{C_1, C_2, \ldots, C_n\}$.
2. Determining the best (B) and worst (W) criteria by the experts. The best criterion include most important or the most desirable criterion, whereas the worst ones include those with the least desirability and/or lowest importance.
3. Determining the priority of the best criteria compared to all the others (the numbers 1 to 9 are used for this purpose). This preference is represented in the form of the following vector:

$$A_B = (\alpha_{B1}, \alpha_{B2,} \ldots, \alpha_{B3}) \quad (6)$$

Here, α_{B1} represents the preference of the best criterion (B) over the criterion j ($\alpha_{BB} = 1$) (Fig. 4).

4. Determining the priority of all the criteria over the worst one (W). The preference vector for this phase is as follows:

$$A_W = (\alpha_{1W}, \alpha_{2W}, \ldots, \alpha_{nW})^T \quad (7)$$

Here, α_{jw} is the preference of the j criterion over the worst one (W) ($\alpha_{ww}=1$) (Fig. 4).

5. Calculating the final weights of the criteria. The following equations are used for this purpose:

$$\text{Min } \varepsilon_i$$

s.t.

$$\left|\frac{W_B}{W_j} - \alpha_{Bj}\right| \leq \varepsilon_i, \forall j = 1,2,\ldots,n$$

$$\left|\frac{W_j}{W_W} - \alpha_{jW}\right| \leq \varepsilon_i, \forall j = 1,2,\ldots,n \quad (8)$$

$$\sum_{j}^{W} W_j = 1$$

$$W_j \geq 0, \forall j = 1,2,\ldots,n$$

The values of the final optimum weights ($W_1^*, W_2^*, \ldots W_n^*$) and ε_i^* are obtained by Equations 8. In addition, the consistency ratio for each criterion can be estimated by using the consistency index table (Table 3) and the ε_i^* value. The following equation states that:

$$\text{Consistency Ratio} = \frac{\varepsilon_i^*}{\text{Consistency Index}} \quad (9)$$

It is evident that the closer the value of the consistency index is to zero, the more realistic the results will be. Refer to Rezaei et al. (2015) for more details of this method.

Adaptive neuro fuzzy inference system (ANFIS)

Although a fuzzy inference system (FIS) using "if-then" rules can analyze complex processes, it is unable to perform the learning process. The adaptive neuro fuzzy inference system (ANFIS) (Jang 1993) is one of the most widely used fuzzy systems for modeling nonlinear problems. This approach, developed by combining a FIS and an artificial neural network (ANN), utilizes the advantages of both approaches to solve problems. The ANN model is able to optimize the fuzzy logic solution through the learning process (Oh and Pradhan 2011). The details of the ANFIS model structure are as follows:

The ANFIS structure was developed by using the Takagi-Sugeno fuzzy rule base (the details are presented in equations 10 and 11).

Rule 1: if x is A_1 and y is B_1 then $f_{1=}p_1x + q_1y + r_1$ (10)

Rule 2: if x is A_2 and y is B_2 then $f_{2=}p_2x + q_2y + r_2$ (11)

Here, x and y are the system inputs and A1, A2, B1 and B2 are fuzzy membership functions. In addition, p_i, q_i and r_i ($\forall$ i = 1, 2) are the parameters of the output function (Jang 1993). In general, the ANFIS structure is made of five layers described below (Fig. 5):

Layer 1: This layer is responsible for the fuzzification of the variables, and the nodes in this layer are adaptive nodes.

$$O_{A_i}^1 = \mu_{A_i}(x), \quad \text{i=1, 2} \tag{12}$$

$$O_{B_i}^1 = \mu_{B_i}(y), \quad \text{i=1, 2} \tag{13}$$

Here, i represents the related node and x and y its input variables, A_i and B_i are linguistic terms and μ_{Ai} (x) and μB_i (y) the membership functions of the node i.

Layer 2: In this section, every node is a fixed node and each one is responsible for multiplying signals entering it. The nodes are named by the Π label and their outputs are as follows (Oh and Pradhan 2011):

$$O_{2,i} = \mu_{A_i}(x).\mu_{B_i}(y) = W_i, \quad for\ i = 1,2 \tag{14}$$

Here, W_i (the so called firing strength of each fuzzy rule) represents each node's output.

Layer 3: This layer has the task of normalizing the output of the second layer. Therefore, the nodes, which are fixed ones and named by the N label, normalize the input values (Equation 15). The numerator of the fraction includes the firing strength of each fuzzy rule, and the denominator includes the total firing strength of each rule.

$$O_{3,i} = \frac{W_i}{W_1+W_2} = \bar{W}_i \ \ for\ i = 1,2 \tag{15}$$

Layer 4: This is considered the second adaptive layer in the ANFIS structure and each node's output is obtained from the following equation:

$$O_{4,i} = \bar{W}_i . f_i = W_i . (p_i x + q_i y + r_i) \quad for\ i = 1,2 \tag{16}$$

In this equation, $\bar{W}_i$ is the normalized firing strength of the third layer. p_i, q_i and r_i are the variable parameters (also referred to as the result parameters) of the node i.

Layer 5: The only node existing in this layer is fixed node labeled Σ. This node sums up all the input signals and calculates the resulting output (Equation 17).

$$O_{5,i} = \sum_i \bar{W}_i f_i = \frac{\sum_i W_i f_i}{\sum_i W_i} \tag{17}$$

For more details on the layers and the algorithms, refer to Jang (1993) and Jang and Sun (1995). Figure 3 shows the process of the study including methods and type of combination used.

Results and Validation

Table 2 shows the weights obtained from the SWARA model and BWM. The values for the slope factor indicate that most of the landslides that occurred in the study area were of the 5-15˚ class with weights of 0.405 and 0.409, respectively. Among the different slope aspects, the north-east aspect, with the values of 0.486 (SWARA) and 0.249 (BWM), had the highest effect on landslide occurrence. In relation to the altitude factor, the 1500-1700 m class had the highest impact on landslide (with values of 0.454 and 0.212 for SWARA and BWM, respectively). The outputs of the SWARA model for the TWI showed that the 5.65-7.31 and 7.31-9.87 classes with values of 0.482 and 0.249, respectively, had the highest probabilities of landslide occurrence. For the BWM, the 5.65-7.31 and 7.31-9.87 classes with the weight of 0.371 had the greatest impact on landslide occurrence. For the plan curvature factor, according to Table 2, the maximum weights obtained from the SWARA and BWM were for the convex class with weights of 0.410 and 0.769, respectively. For the profile curvature factor, the highest SWARA weight (0.489) was that of the concave class and for BWM the highest value (0.470) was that of the concave and convex classes. Results obtained from SWARA indicated that the distance to road, distance to stream and distance to fault in the 0-100 m, 0-100 m and 1200 - 1500 m classes with weights of 0.311, 0.404 and 0.386, respectively, had the highest influence on landslide occurrence. As in the SWARA method, in the BWM also the same classes had the highest weights with the values of 0.397, 0.297 and 0.330, respectively. Concerning lithology, the highest value in the SWARA method (0.344) was that of the Jl class and the highest in the

BWM (0.2) those of the Jl and PlQc classes. For the land use factor, the agriculture class in both models had the strongest relationship with landslide occurrence with values of 0.27 and 0.505, respectively. Landslides were more likely to occur with increases in rainfall. For the precipitation factor, 332.9 - 387.65 mm of rainfall had the highest weights in the SWARA model and BWM (0.352 and 0.647, respectively). In relation to the NDVI factor, the likelihood of landslide occurrence was greatest for the class >0.5 with the weights of 0.356 and 0.574 for the SWARA method and BWM, respectively.

Integration of the ANFIS with SWARA and BWM

In this study, MATLAB was employed to construct the ANFIS model and the SWARA method and BWM to feed it for training the network. For this purpose, all the data were first divided into the training and testing sets. As mentioned earlier 70% of the data (172 landslide locations) were allocated for training and 30% (70 landslide locations) for testing, and they were assigned the value of 1. Using the training data and the SWARA model and BWM, the weights of the sub-criteria were calculated (Table 2). In the next step, 242 non-landslide points, showing the total number of data, were created in the non-landslide areas. Then 0 was allocated to each of them. Out of these non-landslide points, 70% (172) points were selected randomly and considered for training the network. Next, 172 landslide and non-landslide points (with values of 1 and 0) were overlaid upon the conditioning factors and the value of each one was determined. This process was carried out once for the SWARA model and once for the BWM. The values obtained from the overlaying were used as input data for ANFIS training. After ANFIS training using the BWM method and SWARA, all the pixels were entered into MATLAB and the final value of each pixel was determined using the created network. Finally, landslide susceptibility maps were prepared for the hybrid ANFIS-BWM and ANFIS-SWARA models (Fig. 7). The prepared maps were divided into five classes with sensitivity degree of very low, low, moderate, high, and very high. Figure 8 shows the percent area for each class in the ANFIS-SWARA and ANFIS-BWM hybrid models. It is quite clear that the class with very high landslide susceptibility had the lowest area in both LSMs with values of 16.21% and 18.65%, respectively (Table 4). In addition, the classes with high and low landslide susceptibility had the largest areas with the values of. 23.01% and 20.50% for ANFIS-SWARA and ANFIS-BWM, respectively.

Models validation and comparison

Validation is a very important step in estimating the accuracy of a method in producing landslide susceptibility maps. In this study, validation was performed by using 30% of landslide and non-landslide locations (72 points with values of 0 and 1) in two stages. In the first stage, the mean square error was calculated to estimate the accuracy of ANFIS trained network using SWARA and BWM methods. MSE and RMSE are defined as follows:

$$MSE = \frac{1}{n} \sum_{j=1}^{n} (T_j - \bar{T}_j)^2 \quad (18)$$

$$RMSE = \sqrt{\frac{1}{n} \sum_{j=1}^{n} (T_j - \bar{T}_j)^2} \quad (19)$$

where, T_j is the target values and $\bar{T}_j$ is the output values and n is the total number of samples. RMSE is the square root of MSE.

The lower MSE value is (closer to zero) the lower the amount of error in the final prediction and hence the more accuracy the modeling will be. Fig. 6c shows MSE and RMSE for the test dataset. The results showed that the MSE values for the ANFIS-SWARA and ANFIS-BWM models are 0.299 and 0.242, respectively. As the results indicate, the new BWM method outperformed the SWARA model in training the ANFIS.

In the second stage the LSMs were evaluated using the ROC curve. The ROC curve is a graphical representation of the balance between negative and positive error values that can quantitatively estimate the model accuracy. The area under the curve (AUC) illustrates the predicted value of the system by describing its ability in correctly estimating the occurrence of the event (landslide) and the non-occurrence of the event (non-landslide) (Yan et al. 2018). Therefore, the larger the area under (AUC) the curve is the more accurate the model will be and the lower AUC show weak performance of the model. Further details on this curve for validating landslide susceptibility maps are provided in articles by Pourghasemi et al. 2013 and Fan et al. 2017.

In this study, 72 landslide and non-landslide points were overlaid upon the conditioning factors to plot the ROC curves. The values obtained for each point were then used as input data. Figure 9 shows the ROC curves for the methods. In this figure, the areas under the curves for the ANFIS-SWARA and ANFIS-BWM hybrid models are 0.736 and 0.75, respectively. The results obtained from the evaluation of the zoning suggested that both models were able to

predict the landslide prone areas well; however, the ANFIS-BWM model was more accurate and, hence, yielded more reliable outputs.

Discussion

Landslide spatial modeling is a nonlinear and complex problem because it is affected by various parameters. Although there are different methods for landslide susceptibility zoning, the important point is which method or combination of methods should be used, depending on the features of the study area, in order to obtain the best results. The novelty of this study is to produce a new hybrid ANFIS-BWM model and compare it with ANFIS-SWARA to determine the best combination. For this purpose, a database was first developed to contain the inventory map and factors influencing landslides. In the next step, the SWARA and BWM approaches were then executed by using the database and experts' opinions, and the weights of the sub-criteria were determined. The weights obtained from each of the two approaches were entered separately in MATLAB to train ANFIS. After developing the network and calculating the final value of each pixel, the LSMs were generated, and the accuracy of each map was assessed by using the ROC curve. The resultant validation output indicated that the new BWM produced more realistic results than the SWARA method which trained the ANFIS model well and obtained an acceptable output from it. Since bringing the prediction closer to reality is the most important objective in complex environmental issues such as landslides, it is necessary to compare newly introduced methods with the previous ones in order to achieve more optimal results.

The research models have attracted the interest of landslide researchers. Oh and Pradhan. (2011) employed the ANFIS model with the triangular, trapezoidal, Gaussian, 2-sided Gaussian, generalized bell, sigmoid 1, sigmoid 2 and polynomial membership functions for landslide spatial modeling on Penang Island in Malaysia. For this purpose, they first determined the relationships between the eight effective factors and the previous landslides by using the frequency ratio method. The ANFIS model was then implemented in MATLAB and to estimate the values obtained from the frequency ratio method and its accuracy through the ROC curve. They showed that the triangular, trapezoidal, generalized bell and polynomial membership functions were slightly more accurate than the others, although all the membership functions that were used yielded very good results with accuracies higher than 84%. In order landslide spatial modelling for Iran, Dehnavi et al. (2015) integrated the SWARA multi-criteria decision-making approach with the ANFIS method. In the first step, the SWARA model was used to

specify the weights of sub-criteria, and the LSM was then generated. In the second step, the SWARA model weights were utilized to train the ANFIS and generate the map for the hybrid ANFIS-SWARA landslide susceptibility model. They found that the ANFIS-SWARA hybrid model with the area under the curve of 0.8 yielded a more accurate prediction than the SWARA method with the area under the curve of 0.78. Gigovic et al. (2019) integrated the BWM with the WLC and OWA methods for zoning regional landslides in western Serbia. For this purpose, they first created a database that included 15 conditioning factors and 1082 previous landslides. The normalized weights of the effective factors were then calculated by using the BWM. The WLC and OWA methods were then employed to produce LSMs. Finally, the performance of each map was assessed by through the ROC curve. They showed that the OWA method with 94.1% accuracy outperformed the WLC method that had the accuracy of 90.5%.

In this study, the important of using new models to improve the performance of machine learning methods was shown. Based on the results shown in table 2, although both methods are of the type of MCDM and include values between 0 and 0.5, the new BWM model performs better compared to SWARA model. Therefore, the type of model that is used to determine the correlation between conditioning factors and the landslide occurrence is effective in improving the results. According to the research findings, the employed methods performed well in estimating landslide prone areas. In addition, the use of the two ANFIS-BWM and ANFIS-SWARA hybrid models with the accuracies of 75% and 73.6%, respectively, confirmed this statement. It is recommended to integrate SWARA and BWM multi-criteria decision-making models with machine learning methods such as ANFIS for other similar areas.

Conclusion

Known as natural destructive ground-deforming phenomena, landslides have occurred in all historical periods. Evaluation of landslide susceptibility maps is a multistage and complicated process and, therefore, the careful selection and execution of the stages of the model will result in generation of maps yielding better results.

In the present study, a new comparison was drawn between two multi-criteria decision-making methods to train the ANFIS model. For this purpose, it was decided to determine the relationships between landslides and effective factors by using the new BWM and the SWARA model. The weights obtained from both methods were then employed to train the ANFIS. Finally, the landslide susceptibility maps were generated using the ANFIS-SWARA and ANFIS-BWM ensemble models. The results of validation using the ROC curve showed that the ANFIS-BWM model with a 75% prediction accuracy outperformed the ANFIS-SWARA

model with a 73.6% prediction accuracy. Although both the BWM and the SWARA technique were multi-criteria decision-making models, their outputs differed in types of ranking and weighting. Therefore, it is essential to decide the output of which method should be utilized to train a machine learning model. Since these models yielded good results, they are recommended for use in other similar areas because they can substantially help land use managers and planners in making important decisions.

Declarations

Ethics approval and consent to participate.

Not applicable.

Consent for publication

Not applicable.

Availability of data and materials

All data generated or analyzed during this study are confidential.

Competing interests

The authors declare that they have no competing interests.

Funding

Not applicable.

Code availability (software application or custom code)

Not applicable.

Authors' contributions

All authors contributed to the study conception and design. Data collection and material preparation were performed by SP. Development and design of methodology and creation of models were performed by SP and AN. BP consulted for the methodology application. AN was the supervisors of the work. The first draft of the manuscript was written by SP and AN and BP commented on previous versions of the manuscript.

References

Achour Y, Boumezbeur A, Hadji R, Chouabbi A, Cavaleiro V, Bendaoud EA (2017) Landslide susceptibility mapping using analytic hierarchy process and information value methods along a highway road section in Constantine, Algeria. Arab J Geosci. 10:194.

Adineh F, Motamedvaziri B, Ahmadi H, Moeini A (2018) Landslide susceptibility mapping using Genetic Algorithm for the Rule Set Production (GARP) model. J Mt Sci. 15:2013-2026.

Aghdam IN, Pradhan B, Panahi M (2017) Landslide susceptibility assessment using a novel hybrid model of statistical bivariate methods (FR and WOE) and adaptive neuro-fuzzy inference system (ANFIS) at southern Zagros Mountains in Iran. Environ Earth Sci. 76:237.

Ahmad WNKW, Rezaei J, Sadaghiani S, Tavasszy LA (2017) Evaluation of the external forces affecting the sustainability of oil and gas supply chain using Best Worst Method. J Clean Prod. 153:242-252.

Ahmed B (2015) Landslide susceptibility mapping using multi-criteria evaluation techniques in Chittagong Metropolitan Area, Bangladesh. Landslides 12:1077-1095.

Arabameri A, Pradhan B, Rezaei K, Sohrabi M, Kalantari Z (2019) GIS-based landslide susceptibility mapping using numerical risk factor bivariate model and its ensemble with linear multivariate regression and boosted regression tree algorithms. J Mt Sci. 16:595-618.

Baena JAP, Scifoni S, Marsella M, De Astis G, Fernández CI (2019) Landslide susceptibility mapping on the islands of Vulcano and Lipari (Aeolian Archipelago, Italy), using a multi-classification approach on conditioning factors and a modified GIS matrix method for areas lacking in a landslide inventory. Landslides 16:969-982.

Berhane G, Kebede M, Alfarrah N (2020) Landslide susceptibility mapping and rock slope stability assessment using frequency ratio and kinematic analysis in the mountains of Mgulat area, Northern Ethiopia. Bull Eng Geol Environ. 1-17. https://doi.org/10.1007/s10064-020-01905-9

Bui DT, Pradhan B, Lofman O, Revhaug I, Dick OB (2012) Spatial prediction of landslide hazards in Hoa Binh province (Vietnam): a comparative assessment of the efficacy of evidential belief functions and fuzzy logic models. Catena 96:28-40.

Bui DT, Tuan TA, Klempe H, Pradhan B, Revhaug I (2016) Spatial prediction models for shallow landslide hazards: a comparative assessment of the efficacy of support vector machines, artificial neural networks, kernel logistic regression, and logistic model tree. Landslides 13:361-378.

Chalkias C, Ferentinou M, Polykretis C (2014) GIS-based landslide susceptibility mapping on the Peloponnese Peninsula, Greece. Geosciences 4:176-190.

Colkesen I, Sahin EK, Kavzoglu T (2016) Susceptibility mapping of shallow landslides using kernel-based Gaussian process, support vector machines and logistic regression. J Afr Earth Sci. 118:53-64.

Conforti M, Pascale S, Robustelli G, Sdao F (2014) Evaluation of prediction capability of the artificial neural networks for mapping landslide susceptibility in the Turbolo River catchment (northern Calabria, Italy). Catena 113:236-250.

Cui K, Lu D, Li W (2017) Comparison of landslide susceptibility mapping based on statistical index, certainty factors, weights of evidence and evidential belief function models. Geocarto Int. 329:935-955.

Dehnavi A, Aghdam IN, Pradhan B, Varzandeh MHM (2015) A new hybrid model using step-wise weight assessment ratio analysis (SWARA) technique and adaptive neuro-fuzzy inference system (ANFIS) for regional landslide hazard assessment in Iran. Catena 135:122-148.

Ding Q, Chen W, Hong H (2017) Application of frequency ratio, weights of evidence and evidential belief function models in landslide susceptibility mapping. Geocarto Int. 32:619-639.

571 Dou J, Oguchi T, Hayakawa YS, Uchiyama S, Saito H, Paudel U (2014) GIS-based landslide
572 susceptibility mapping using a certainty factor model and its validation in the Chuetsu Area,
573 Central Japan. In Landslide science for a safer geoenvironment. p. 419-424.
574
575 Du G, Zhang Y, Yang Z, Guo C, Yao X, Sun D (2019) Landslide susceptibility mapping in the
576 region of eastern Himalayan syntaxis, Tibetan Plateau, China: a comparison between analytical
577 hierarchy process information value and logistic regression-information value methods. Bull
578 Eng Geol Environ. 78(6):4201-4215.
579
580 Erener A, Düzgün HSB (2010) Improvement of statistical landslide susceptibility mapping by
581 using spatial and global regression methods in the case of More and Romsdal
582 (Norway). Landslides 7:55-68.
583
584
585 Erener A, Mutlu A, Düzgün HS (2016) A comparative study for landslide susceptibility
586 mapping using GIS-based multi-criteria decision analysis (MCDA), logistic regression (LR)
587 and association rule mining (ARM). Eng Geol. 203:45-55.
588
589 Fan W, Wei XS, Cao YB, Zheng, B (2017) Landslide susceptibility assessment using the
590 certainty factor and analytic hierarchy process. J Mt Sci. 14:906-925.
591
592 Farrokhnia A, Pirasteh S, Pradhan B, Pourkermani M, Arian M (2011) A recent scenario of
593 mass wasting and its impact on the transportation in Alborz Mountains, Iran using geo-
594 information technology. Arab J Geosci. 4:1337-1349.
595
596 Feizizadeh B, Roodposhti MS, Blaschke T, Aryal J (2017) Comparing GIS-based support
597 vector machine kernel functions for landslide susceptibility mapping. Arab J Geosci. 10:122.
598
599 Gigović L, Drobnjak S, Pamučar D (2019) The application of the hybrid GIS spatial multi-
600 criteria decision analysis best – worst methodology for landslide susceptibility
601 mapping. ISPRS Int J Geo-Inf. 8:79.
602
603 Gutiérrez F, Linares R, Roqué C, Zarroca M, Carbonel D, Rosell J, Gutiérrez M (2015) Large
604 landslides associated with a diapiric fold in Canelles Reservoir (Spanish Pyrenees): Detailed

geological – geomorphological mapping, trenching and electrical resistivity imaging. Geomorphology 241:224-242.

Grabs T, Seibert J, Bishop K, Laudon H (2009) Modeling spatial patterns of saturated areas: A comparison of the topographic wetness index and a dynamic distributed model. J Hydrol. 373:15-23.

Hall FG, Townshend JR, Engman ET (1995) Status of remote sensing algorithms for estimation of land surface state parameters. Remote Sens. Environ. 51:138-156.

Hong H, Chen W, Xu C, Youssef AM, Pradhan B, Tien Bui D (2017) Rainfall-induced landslide susceptibility assessment at the Chongren area (China) using frequency ratio, certainty factor, and index of entropy. Geocarto Int. 322:139-154.

Jang JS (1993) ANFIS: adaptive-network-based fuzzy inference system. IEEE Trans. Syst. Man Cybern. 23:665-685.

Juliev M, Mergili M, Mondal I, Nurtaev B, Pulatov A, Hübl J (2019) Comparative analysis of statistical methods for landslide susceptibility mapping in the Bostanlik District, Uzbekistan. Sci Total Environ. 653:801-814.

Kavzoglu T, Sahin EK, Colkesen I (2014) Landslide susceptibility mapping using GIS-based multi-criteria decision analysis, support vector machines, and logistic regression. Landslides. 11:425-439.

Kayastha P, Dhital MR, De Smedt F (2012) Landslide susceptibility mapping using the weight of evidence method in the Tinau watershed, Nepal. Nat Hazards. 63:479-498.

Keršulienė V, Turskis Z (2011) Integrated fuzzy multiple criteria decision-making model for architect selection. Technol. Econ Dev Econ. 17:645-666.

Kim JC, Lee S, Jung HS, Lee S (2018) Landslide susceptibility mapping using random forest and boosted tree models in Pyeong-Chang, Korea. Geocarto Int. 339:1000-1015.

639 Kouli M, Loupasakis C, Soupios P, Rozos D, Vallianatos F (2014) Landslide susceptibility
640 mapping by comparing the WLC and WofE multi-criteria methods in the West Crete Island,
641 Greece. Environ Earth Sci. 72:5197-5219.
642
643 Kumar S, Srivastava PK, Snehmani (2017) GIS-based MCDA-AHP modeling for avalanche
644 susceptibility mapping of Nubra valley region, Indian Himalaya. Geocarto Int. 32:1254-1267.
645
646 Lin L, Lin Q (2017) Landslide susceptibility mapping on a global scale using the method of
647 logistic regression. Nat Hazards Earth Syst. Sci. 17:1411-1424.
648
649 Mardani A, Zavadskas EK, Khalifah Z, Zakuan N, Jusoh A, Nor KM, Khoshnoudi M (2017)
650 A review of multi-criteria decision-making applications to solve energy management
651 problems: Two decades from 1995 to 2015. Renew Sust Energ Rev. 71: 216-256.
652
653 Moayedi H, Mehrabi M, Mosallanezhad M, Rashid ASA, Pradhan B (2019) Modification of
654 landslide susceptibility mapping using optimized PSO-ANN technique. Eng Comput. 35:967-
655 984.
656
657 Moosavi V, Niazi Y (2016) Development of hybrid wavelet packet-statistical models (WP-
658 SM) for landslide susceptibility mapping. Landslides 13:97-114.
659
660 Nadim F, Kjekstad O, Peduzzi P, Herold C, Jaedicke C (2006) Global landslide and avalanche
661 hotspots. Landslides 3:159-173.
662
663 Oh HJ, Pradhan B (2011) Application of a neuro-fuzzy model to landslide-susceptibility
664 mapping for shallow landslides in a tropical hilly area. Comput Geosci. 37:1264-1276.
665
666 Oh HJ, Kadavi PR, Lee CW, Lee S (2018) Evaluation of landslide susceptibility mapping by
667 evidential belief function, logistic regression and support vector machine models. GEOMAT
668 Nat Haz Risk. 9:1053-1070.
669
670 Paryani S, Neshat A, Javadi S, Pradhan B (2020) Comparative performance of new hybrid
671 ANFIS models in landslide susceptibility mapping. Nat Hazards. 1-28.
672 https://doi.org/10.1007/s11069-020-04067-9

673
674 Pham, B. T., Bui, D. T., Pourghasemi, H. R., Indra, P., & Dholakia, M. B. (2017). Landslide
675 susceptibility assesssment in the Uttarakhand area (India) using GIS: a comparison study of
676 prediction capability of naïve bayes, multilayer perceptron neural networks, and functional
677 trees methods. Theoretical and Applied Climatology, 128(1-2), 255-273.
678
679 Pham BT, Prakash I (2018) Machine learning methods of kernel logistic regression and
680 classification and regression trees for landslide susceptibility assessment at part of Himalayan
681 area, India. Indian J Sci Technol. 11:1-11.
682
683 Pham BT, Prakash I (2019) Evaluation and comparison of LogitBoost Ensemble, Fisher's
684 Linear Discriminant Analysis, logistic regression and support vector machines methods for
685 landslide susceptibility mapping. Geocarto Int 34:316-333.
686
687 Polykretis C, Ferentinou M, Chalkias C (2015) A comparative study of landslide susceptibility
688 mapping using landslide susceptibility index and artificial neural networks in the Krios River
689 and Krathis River catchments (northern Peloponnesus, Greece). Bull Eng Geol Environ. 74(1),
690 27-45.
691
692 Polykretis C, Chalkias C, Ferentinou M (2019) Adaptive neuro-fuzzy inference system
693 (ANFIS) modeling for landslide susceptibility assessment in a Mediterranean hilly area. B Eng
694 Geol Environ. 78:1173-1187.
695
696 Pourghasemi HR, Moradi HR, Aghda SF (2013) Landslide susceptibility mapping by binary
697 logistic regression, analytical hierarchy process, and statistical index models and assessment
698 of their performances. Nat Hazards. 69:749-779.
699
700 Pourghasemi, H. R., & Rossi, M. (2017). Landslide susceptibility modeling in a landslide prone
701 area in Mazandarn Province, north of Iran: a comparison between GLM, GAM, MARS, and
702 M-AHP methods. Theoretical and Applied Climatology, 130(1-2), 609-633.
703
704 Pradhan B (2011) Manifestation of an advanced fuzzy logic model coupled with Geo-
705 information techniques to landslide susceptibility mapping and their comparison with logistic
706 regression modelling. Environ Ecol Stat. 18:471-493.

Pradhan B (2013) A comparative study on the predictive ability of the decision tree, support vector machine and neuro-fuzzy models in landslide susceptibility mapping using GIS. Comput Geosci. 51:350-365.

Pradhan B, Seeni MI, Kalantar B (2017) Performance evaluation and sensitivity analysis of expert-based, statistical, machine learning, and hybrid models for producing landslide susceptibility maps. In: Laser scanning applications in landslide assessment. Springer international publishing, pp. 193-232. Springer, Cham.

Umar Z, Pradhan B, Ahmad A, Jebur MN, Tehrany MS (2014) Earthquake induced landslide susceptibility mapping using an integrated ensemble frequency ratio and logistic regression models in West Sumatera Province, Indonesia. Catena 118:124-135.

Ramesh V, Anbazhagan S (2015) Landslide susceptibility mapping along Kolli hills Ghat road section (India) using frequency ratio, relative effect and fuzzy logic models. Environ Earth Sci. 73:8009-8021.

Regmi AD, Devkota KC, Yoshida K, Pradhan B, Pourghasemi HR, Kumamoto T, Akgun A (2014) Application of frequency ratio, statistical index, and weights-of-evidence models and their comparison in landslide susceptibility mapping in Central Nepal Himalaya. Arab J Geosci. 7:725-742.

Rezaei J (2015) Best-worst multi-criteria decision-making method. Omega 53:49-57.

Rozos D, Pyrgiotis L, Skias S, Tsagaratos P (2008) An implementation of rock engineering system for ranking the instability potential of natural slopes in Greek territory. An application in Karditsa County. Landslides 5:261-270.

Sharma S, Mahajan AK (2019) A comparative assessment of information value, frequency ratio and analytical hierarchy process models for landslide susceptibility mapping of a Himalayan watershed, India. Bull Eng Geol Environ 78(4):2431-2448.

Turan, İ. D., Özkan, B., Türkeş, M., & Dengiz, O. (2020). Landslide susceptibility mapping for the Black Sea Region with spatial fuzzy multi-criteria decision analysis under semi-humid and humid terrestrial ecosystems. Theoretical and Applied Climatology, 1-14.

Wang LJ, Guo M, Sawada K, Lin J, Zhang J (2015) Landslide susceptibility mapping in Mizunami City, Japan: A comparison between logistic regression, bivariate statistical analysis and multivariate adaptive regression spline models. Catena 135:271-282.

Xiao T, Yin K, Yao T, Liu S (2019) Spatial prediction of landslide susceptibility using GIS-based statistical and machine learning models in Wanzhou County, Three Gorges Reservoir, China. Acta Geochimica, 38:654-669.

Yan F, Zhang Q, Ye S, Ren B (2019) A novel hybrid approach for landslide susceptibility mapping integrating analytical hierarchy process and normalized frequency ratio methods with the cloud model. Geomorphology 327:170-187.

Youssef, A. M., Pradhan, B., Jebur, M. N., & El-Harbi, H. M. (2015). Landslide susceptibility mapping using ensemble bivariate and multivariate statistical models in Fayfa area, Saudi Arabia. Environmen. Earth Sci. 73:3745-3761.

Zhang G, Cai Y, Zheng Z, Zhen J, Liu Y, Huang K (2016) Integration of the statistical index method and the analytic hierarchy process technique for the assessment of landslide susceptibility in Huizhou, China. Catena 142:233-244.

Zhu AX, Miao Y, Wang R, Zhu T, Deng Y, Liu J, Lin y, Qin CZ, Hong H (2018) A comparative study of an expert knowledge-based model and two data-driven models for landslide susceptibility mapping. Catena 166:317-327.

Figures

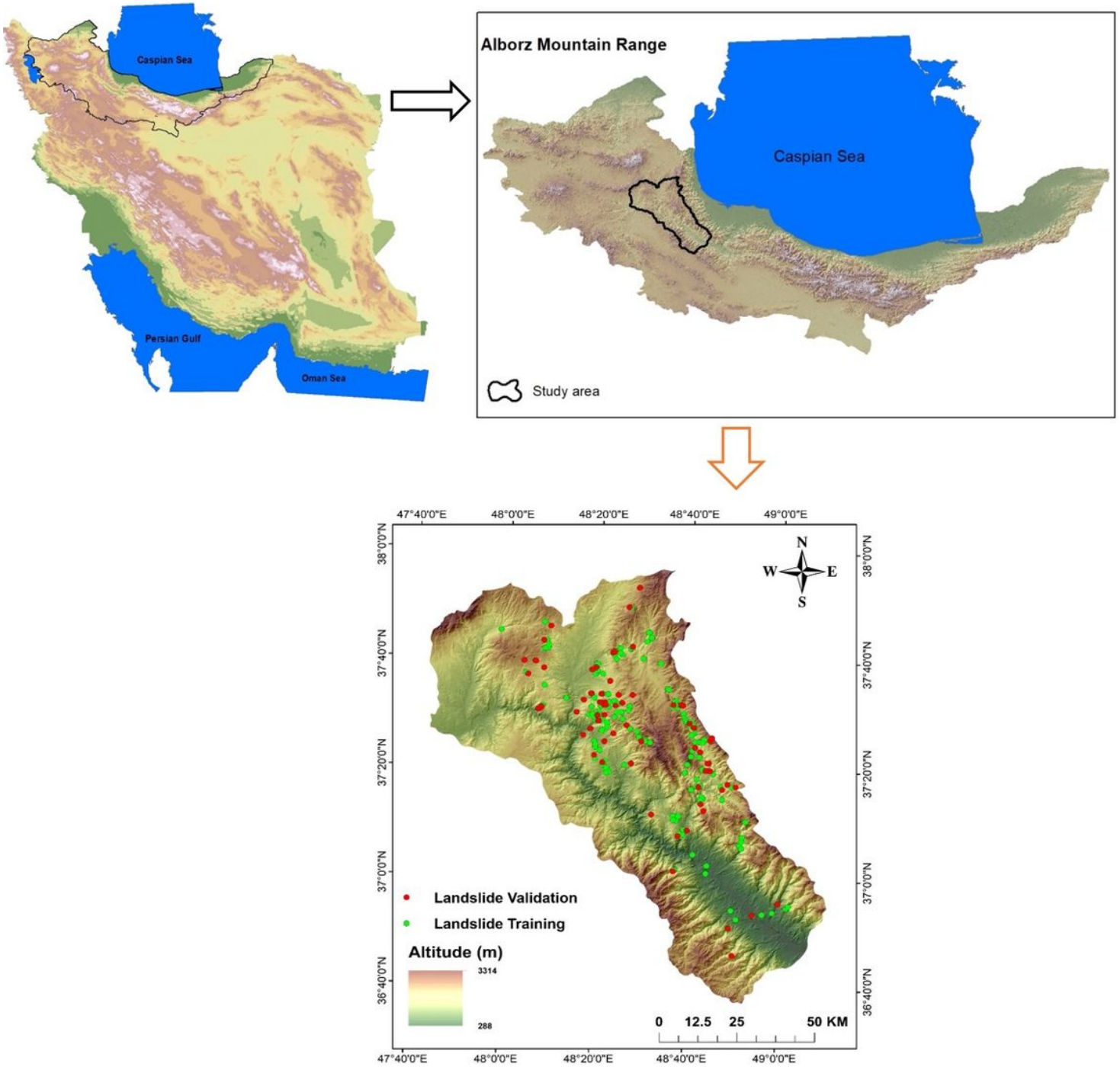

Figure 1

Location of the study area

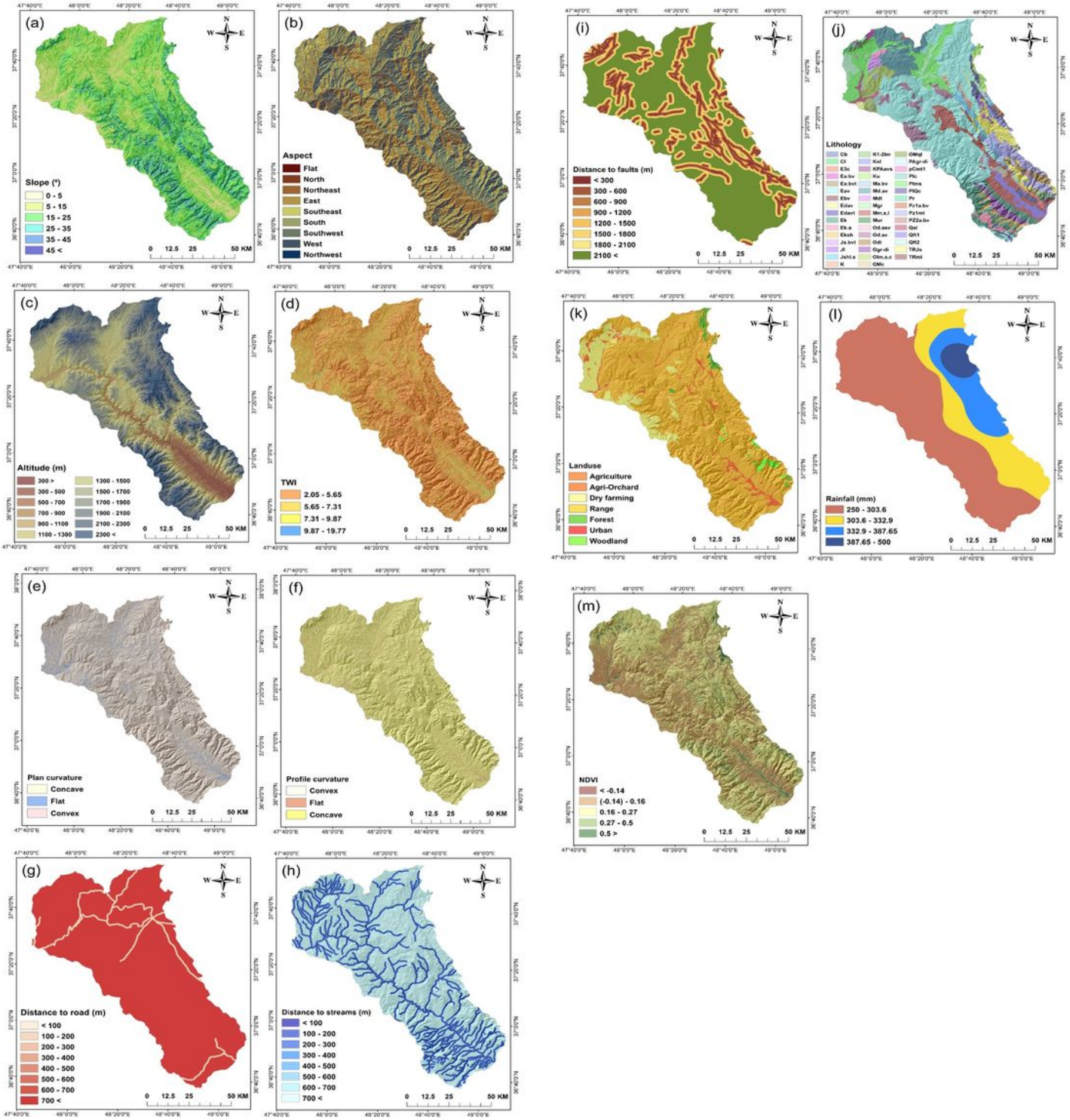

Figure 2

Produced conditioning factors of the study; a, slope angle; b, slope aspect; c, altitude; d, TWI; e, plan curvature; f, profile curvature; g, distance to roads; h, distance to streams; i, distance to faults; j, lithology; k, land use; l, rainfall; m, NDVI

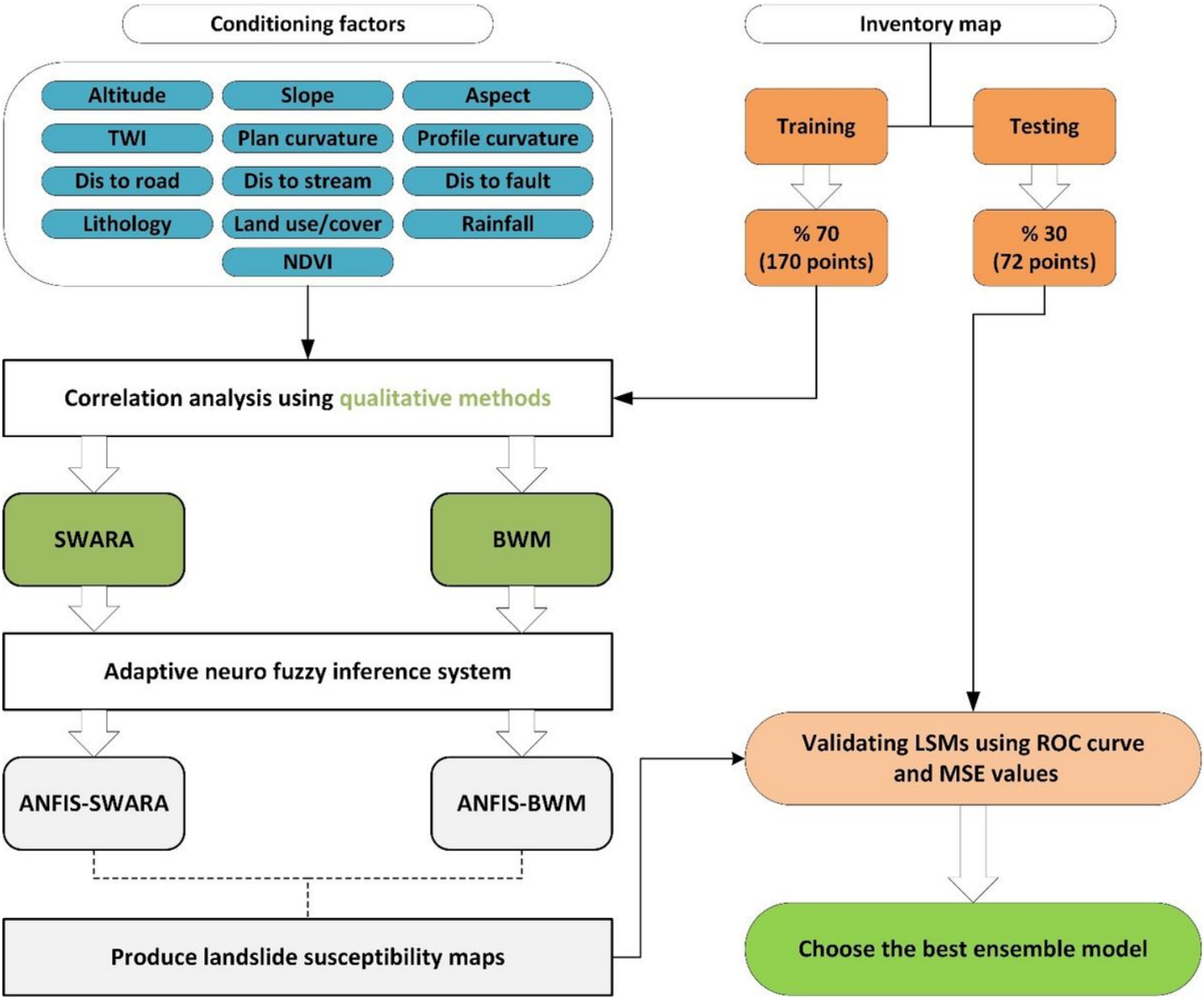

Figure 3

Flowchart of the study that showing all steps

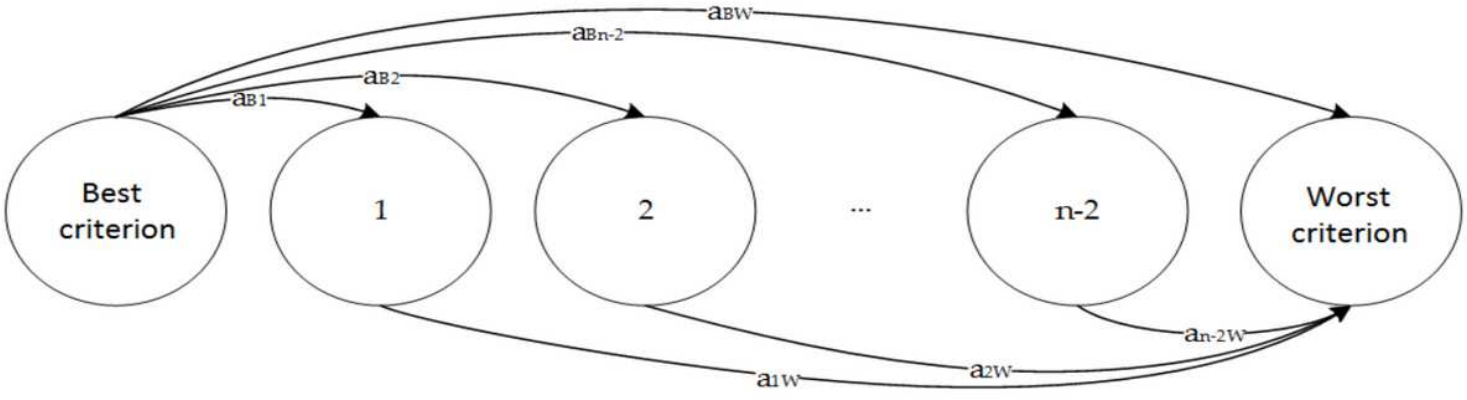

Figure 4

Reference comparison for BWM model

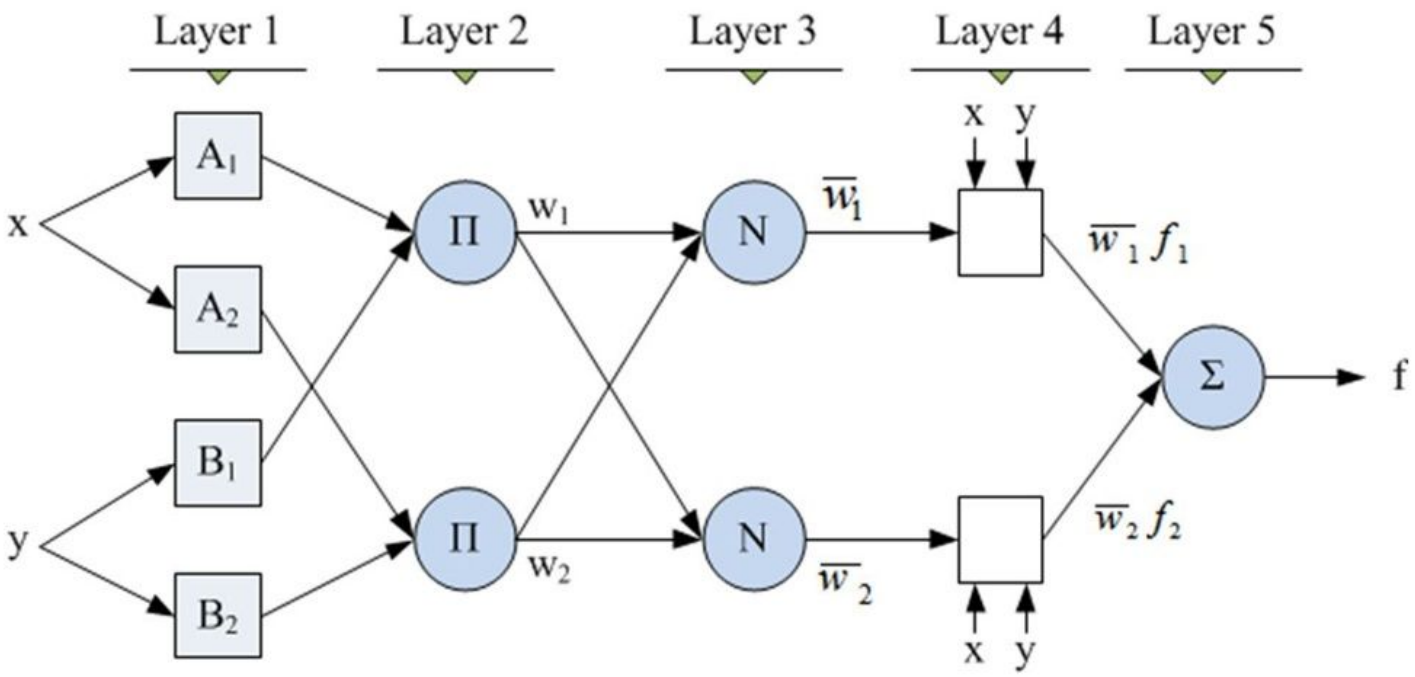

Figure 5

The structure of ANFIS model

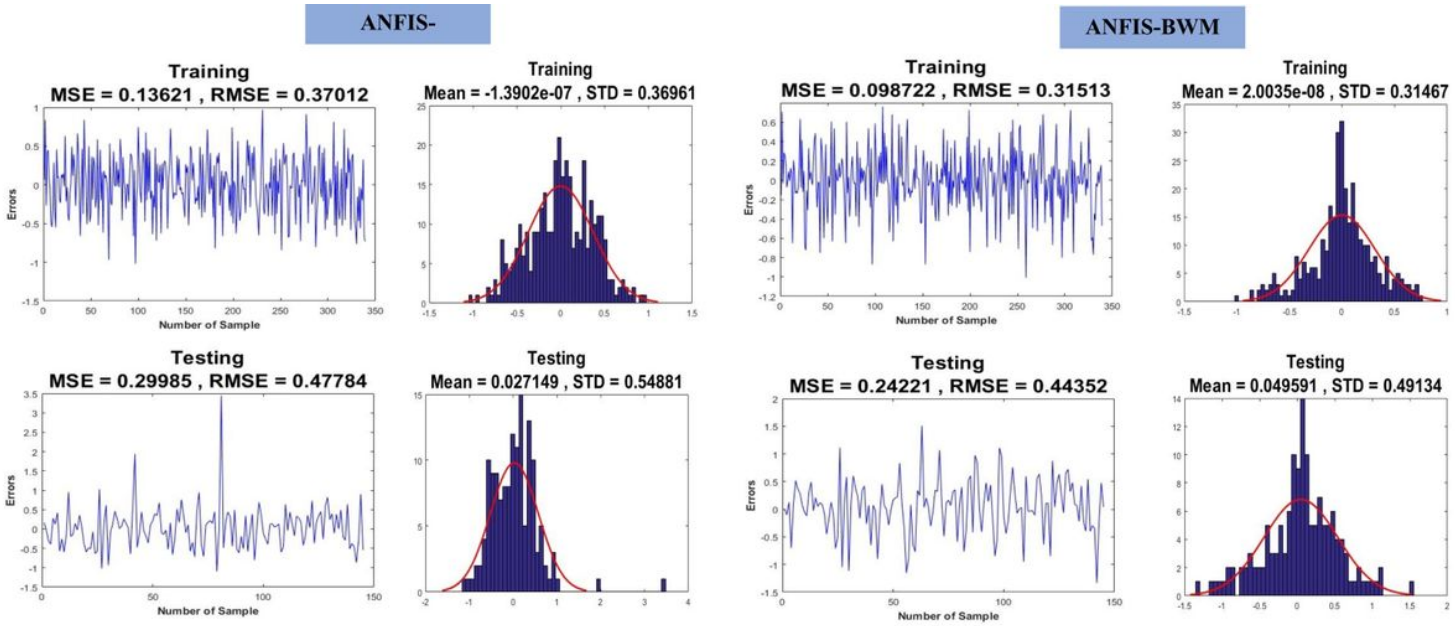

Figure 6

ANFIS-SWARA and ANFIS-BWM training and testing datasets a) MSE and RMSE value in the training phase; b) frequency errors in the training phase; c) MSE and RMSE value in the testing phase d) frequency errors in the testing phase

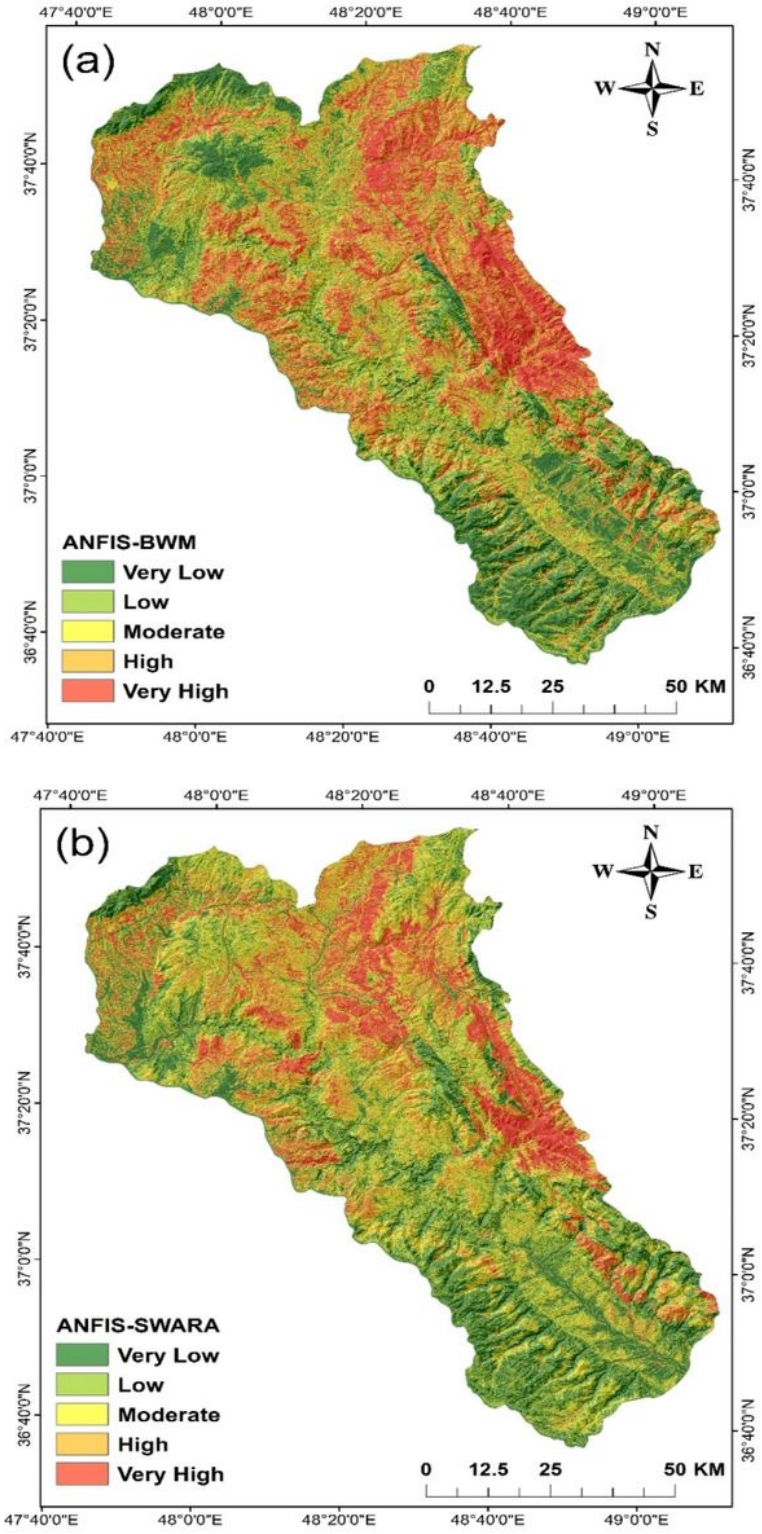

Figure 7

Landslide susceptibility map produced by ANFIS-BWM (a) and ANFIS-SWARA (b) models

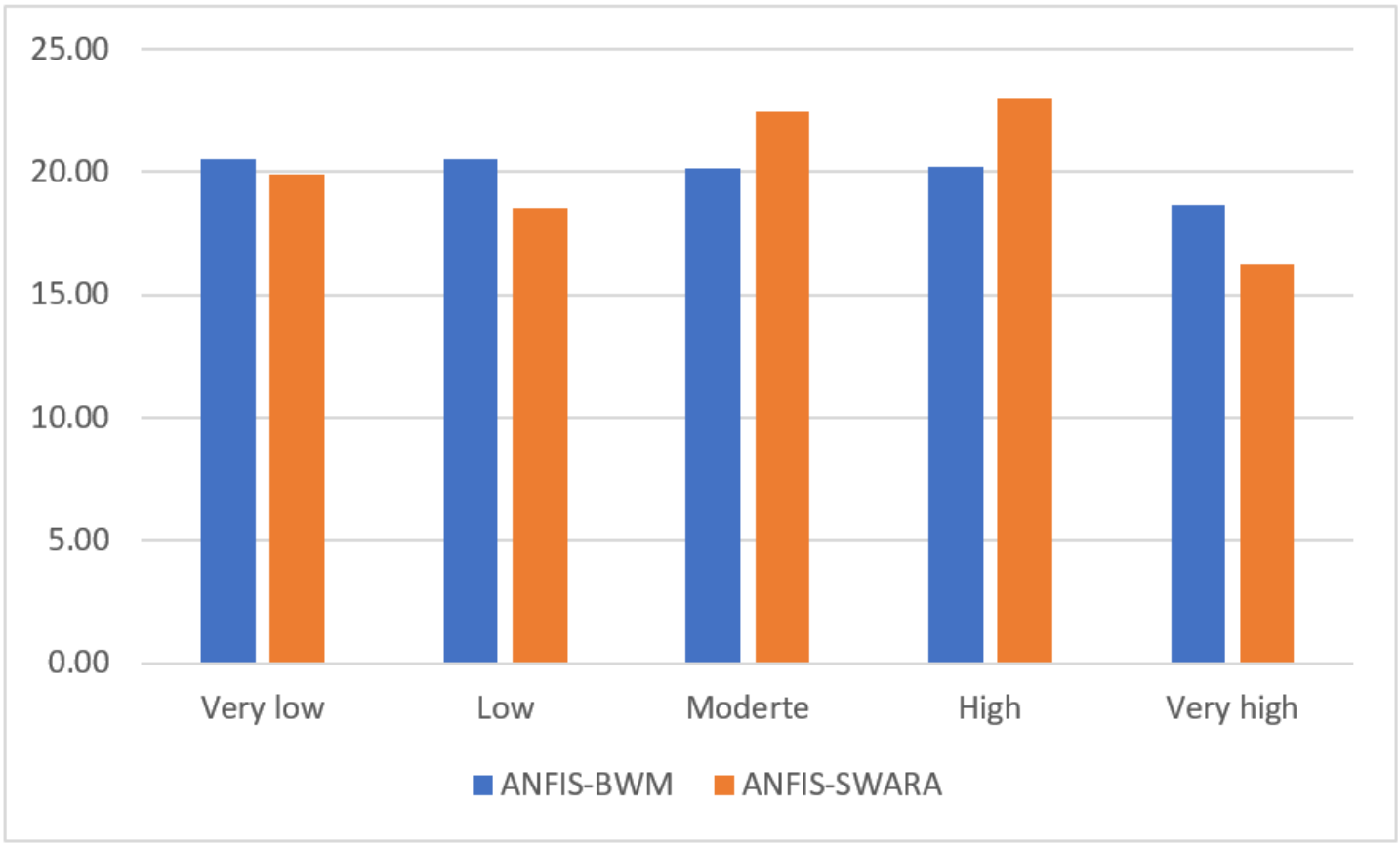

Figure 8

Percentages of landslide susceptibility classes

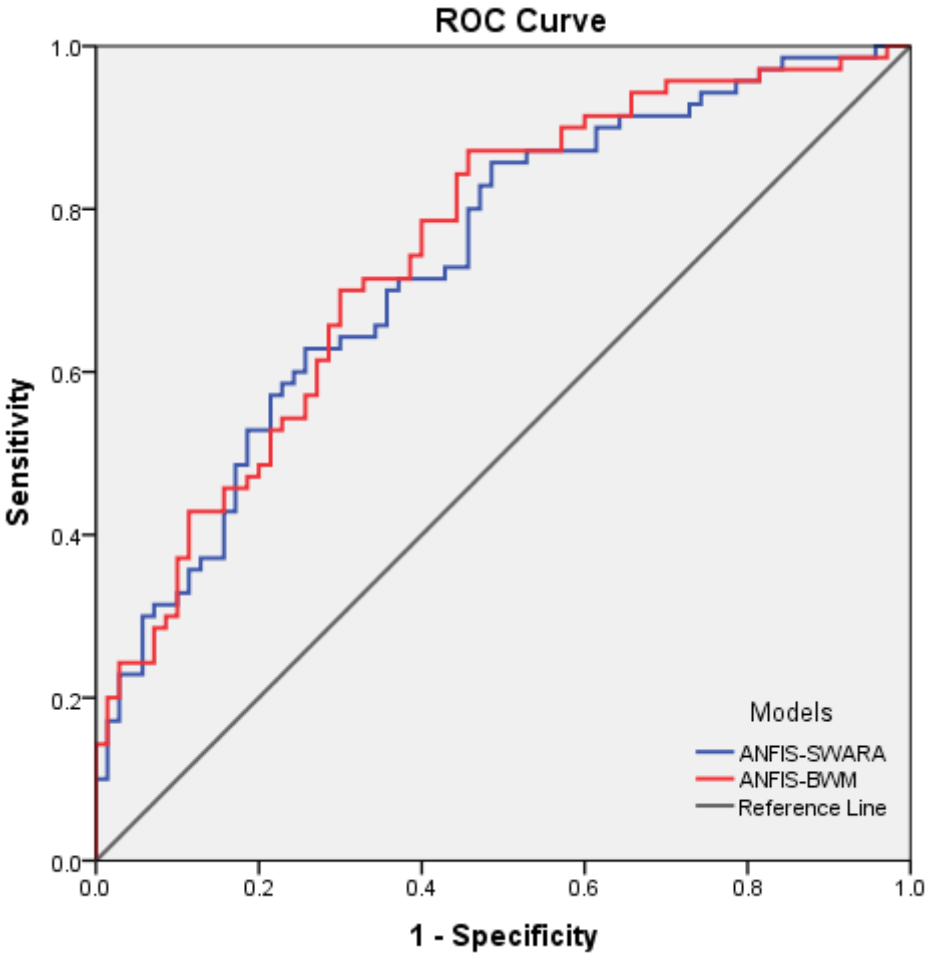

Figure 9

receiver operating characteristic curve for validation

Supplementary Files

This is a list of supplementary files associated with this preprint. Click to download.

- GraphicalAbstract.docx
- Highlight.docx